Research Journal of Engineering Sciences ISSN 2278 – 9472
Vol. **1(3),** 38-44, Sept. **(2012)** *Res. J. Engineering Sci.*

Investigation of Superresolution using Phase based Image Matching with Function Fitting

Budi Setiyono[1], Mochamad Hariadi[2] and Mauridhi Hery Purnomo[2]
[1]Department of Mathematics, Sepuluh Nopember Institute of Technology, Surabaya, INDONESIA
[2]Department of Electrical Engineering, Sepuluh Nopember Institute of Technology, Surabaya, INDONESIA

Available online at: www.isca.in
Received 4th September 2012, revised 11th September 2012, accepted 14th September 2012

Abstract

Higher resolution image provide more detail information, so that it obtain more accurate image analysis. Many areas require high resolution image, such as medical, sensing satellite, image of the telescope and pattern recognition. This research make a process to obtain high resolution images, known as superresolution. This superresolution using a series of images in the same scene as the reference image. Two main stages in the super resolution are the registration and reconstruction. This research propose a composite between Phase-Based Image Matching (PBIM) registration, and reconstruction using structure - adaptive normalized convolution algorithm (SANC) and projection onto convext sets algorithm (POCs). PBIM was used to estimate translational registration stage. We used the function fitting around the peak point, to obtain sub pixel accurate shift. The results of this registration were used for reconstruction. Two registration method and reconstruction algorithms have been tested to obtain the most appropriate composite by measuring the value of peak signal to noise ratio (PSNR). In determining the effect of registration and reconstruction of objects which have different characteristics, we used some images that contain lots of texture and some other with less texture. The result showed that the composite of PBIM and reconstruction with POCs algorithm has the highest average of PSNR for both characteristics images. Images with lots of texture have PSNR average of 32.1606, while PSNR average of images with less texture was 29.99313. For every collaborative algorithm that has been tested, images with less texture have lower average of PSNR than ones with lots of texture. In this experiment, PBIM registration with function fitting has an average PSNR value of 2.88% higher than the Keren registration.

Keywords: Phased based image matching, reconstruction, registration, superresolution.

Introduction

Nowadays image processing becomes quite important in human life. High Resolution Image provides more detail information, so that the analysis of image becomes more accurate. For instance of high resolution, medical images will help physicians to make appropriate diagnosis. The higher resolution images provide more detailed information. Image with high resolution can be obtained by improving the quality of the CCD, but it is costly. Another approach is the superresolution. It is done by processing the signal, that require lower cost.

Superresolution (SR) is a method to improve the resolution of low resolution images (LR) into high resolution image (HR). Based on the number of reference images are used, superresolution can be grouped into two categories. They are superresolution using an image, and superresolution using multiple images in the same scene as reference[1]. Superresolution has two main stages, which are the registration and reconstruction. Some researches showed that the good reconstructions were strongly influenced by the registration process[1-3]. Phase Based Image Matching (PBIM) was used to estimate the translational registration stage, because of its high accuracy. Only translation with sub pixel accuracy that contributed in the reconstruction process[4-6]. The research also showed that PBIM was better in performance, efficiency and complexity compared to the block-matching method.

Other researchers compared two registration techniques, algorithms based on nonlinear optimization and Discrete Fourier transform (DFTs). The results showed that after being compared with usual FFT approach, these algorithms have shorter computational time and also required less memory[7,8].

Superresolution: The registration and reconstruction images are two main stages of superresolution. The registration is done by estimating the pixels translation, which is useful for reconstruction. If the translation pixels are in integer, then each image will contain the same information. This cannot be used in superresolution. But if the translation level are in real pixels (sub pixels), it will obtain additional information that will be useful at the time of reconstruction. Figure 1 shows the step of the superresolution.

Phase based Image Matching: Suppose there are two images $\boldsymbol{f(n_1, n_2)}$ and $\boldsymbol{g(n_1, n_2)}$ with dimensions $\boldsymbol{N_1 x N_2}$. Assumed index $\boldsymbol{n_1}$ ranged from $\boldsymbol{-M_1, \dots, M_1}$and $\boldsymbol{n_2}$ ranged from $\boldsymbol{-M_2, \dots, M_2}$. To simplify these indexes we used the

equations $\boldsymbol{N_1 = 2M_1 + 1}$ and $\boldsymbol{N_2 = 2M_2 + 1}$. Discrete Fourier transform of image is :

$$\boldsymbol{F(k_1, k_2) = \sum_{n_1 n_2} f(n_1, n_2) W_{N_1}^{k_1 n_1} W_{N_2}^{k_2 n_2} = A_{F(k_1,k_2)} e^{j\theta_F(k_1,k_2)}} \quad (1)$$

$$\boldsymbol{G(k_1, k_2) = \sum_{n_1 n_2} g(n_1, n_2) W_{N_1}^{k_1 n_1} W_{N_2}^{k_2 n_2} = A_{G(k_1,k_2)} e^{j\theta_F(k_1,k_2)}} \quad (2)$$

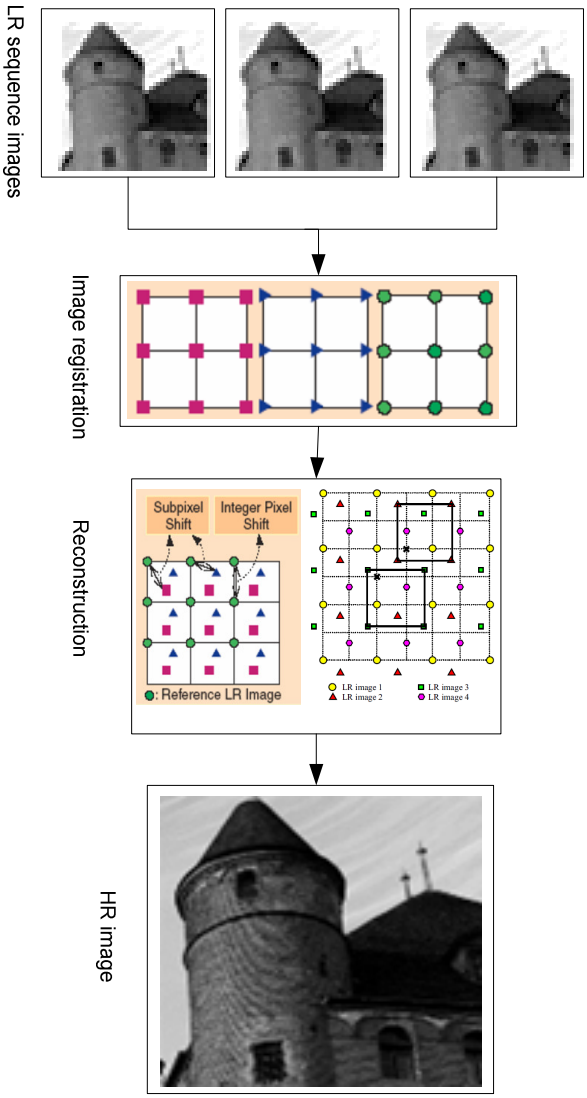

Figure-1
The step of the Superresolution

In this case $F(k_1, k_2)$ and $G(k_1, k_2)$ denote Discrete Fourier Transforms (DFT) from spatial domain $f(n_1, n_2)$ and $g(n_1, n_2)$, $n_1$and n_2 are elemen index in spatial domain at$f(n_1, n_2)$, $k_1 = -M_1, \dots, M_1$, $k_1 = -M_2, \dots, M_2$; $A_{F(k_1,k_2)}$ and $A_{G(k_1,k_2)}$ is the amplitude component; $e^{j\theta_F(k_1,k_2)}$and $e^{j\theta_G(k_1,k_2)}$ are the phase component.

$W_{N_1} = e^{j\frac{2\pi}{N_1}}$ and $W_{N_2} = e^{j\frac{2\pi}{N_2}}$

Cross spectrum phase $\hat{R}(k_1, k_2)$ defined in equation (3) as

$$\hat{R}(k_1, k_2) = \frac{F(k_1,k_2)\overline{G(k_1,k_2)}}{|F(k_1,k_2)\overline{G(k_1,k_2)}|} = e^{j\theta(k_1,k_2)} \quad (3)$$

Phase-Based 2D Inverse of a function $\hat{R}(k_1, k_2)$ shown in the following equation :

$$\hat{r}(n_1, n_2) = \frac{1}{N_1 N_2} \sum_{k_1 k_2} \hat{R}(k_1, k_2) W_{N_1}^{-k_1 n_1} W_{N_2}^{-k_2 n_2} \quad (4)$$

The results of Phase-Based Functions for the function $f(n_1, n_2)$and $g(n_1, n_2)$ which images are identical, it is obtained height of the dominant graph as shown above. While for the function which images are not identical, it is obtained graph that do not have the dominant height.

Fitting Function: Image processed using a computer is a digital image. During the digitizing process, many of information will be lost, such as pixels translation. At continuous images, pixels translation are in the form of real number, but after digitizing, real translation information is lost. Therefore, we need another method to get the actual translation. In the sub-pixel shift correlation phase will be sought by means of interpolation around the peak position. Fitting the function used to obtain the actual peak position, namely :

$$\hat{r}(n_1, n_2) \cong \frac{\alpha}{N_1 N_1} \frac{sin\{\pi(n_1+\delta_1)\}}{sin\left\{\frac{\pi}{N_1}(n_1+\delta_1)\right\}} \frac{sin\{\pi(n_2+\delta_2)\}}{sin\left\{\frac{\pi}{N_2}(n_2+\delta_2)\right\}} \quad (5)$$

Fitting is done using least square, to get the values of $\delta_1$and δ_2 which are the shifting in the subpixel level.

Image Reconstruction: After a series of low-resolution image was registered to obtain the displacement of pixels, then the parameters translational and rotational displacement the images will be used for the reconstruction process. One image in a series of low-resolution image will be used as a reference in the reconstruction. Translational and rotational parameters values pixel displacement is used for projection on a grid of high resolution image. In the next section it will be reviewed the reconstruction algorithms, SANC and POCs algorithms.

Several popular and powerful reconstruction algorithms that have been developed are the Structure-Adaptive Normalized convolution SANC[9,10]. The Structure-Adaptive Normalized convolution (SANC) algorithm is the image interpolation algorithms that work on the scope of normalized convolution. This algorithm defines the applicable function based on the distance to the neighboring pixel point. Other reconstruction algorithm is the Projection onto Convex Sets (POCs). The algorithm is effective for the reconstruction of image containing motion blur and has noise[11,12].

Structure-Adaptive Normalized Convolution (SANC) Algorithm: SANC algorithm is an image interpolation algorithm that works on the scope of Normalized convolution. The next process searches basic functions derived from the value of certainty in these images. After that the values are

operated by equation (6). The operation is the normalized convolution process.

$$p = (B^T W B)^{-1} B^T W f \quad (6)$$

To create sharper image, the process should be repeated, but with the addition of other parameters, such as estimate local image structure and scale. Therefore, these parameters must be known in advance and then made into image density. In addition, the function is created using Gaussian applicability function anisotropic. This iteration process is called the Structure Adaptive Normalized convolution.

Normalized convolution is a technique to modelling the projection of the local signals into a single set of basis functions. Although there are lots of basis functions that can be used, but the commonly used basis functions is the polynomial basis $\{1,x,y,x^2,y^2,xy,...\}$, where 1=$[11\ldots]^T$ (*N series*), $x=[x_1 x_2 .... x_N]^T$, $x_2=[x_{12} x_{22} .... x_{N2}]^T$ and so forth, which reconstructed from the local coordinates of N samples of input.

The use of polynomial basis functions makes Normalized convolution become the same with the expanded local Taylor series. The center of local neighbourhood is in the equation S_0= (x_0,0), while the intensity value is in the position of s = (x+x_0,y+y_0) that approximated by an extended polynomial.

$$\hat{f}(s, s_0) = p_0(s_0) + p_1(s_0)x + p_2(s_0)y + p_3(s_0)x^2 + p_4(s_0)xy + p_1(s_0)y^2 \quad (7)$$

Where (x,) is the local coordinates of the samples associated with the center s_0. (s_0) = [$p_0 p_1 p_2$ .....p_m]. s_0 is the projection coefficient of the polynomial basis function relationships at s_0. Adaptive Structures Normalized convolution system uses the information on the structure and distance between the actual image data input to increase the level of the Normalized convolution.

The equation (8) and (9) below are used to obtain Gradient the Structure Tensor (GST) in order to build an adaptive kernel in pixels output in the local structure of image.

$$GST = \overline{\nabla I \nabla I^T} = \begin{bmatrix} \overline{I_x^2} & \overline{I_x I_y} \\ I_x I_y & \overline{I_y^2} \end{bmatrix} = \lambda_u u u^T + \lambda_v v v^T \quad (8)$$

$$\emptyset = \arg(u), A = \frac{\lambda_u - \lambda_v}{\lambda_u + \lambda_v} \quad (9)$$

$\emptyset$ is main axis and A is the intensity of the anisotropic, both of them are calculated from the eigenvector u, v that correspond to the eigenvalue ($\lambda_u \geq \lambda_v$), where$I_x = \partial I/\partial x$ and $I_y = \partial I/\partial y$ is the gradient correspondent. Other important characteristics of the data are the local sample density, because it illustrates how much information that available at grid points near the high-resolution.

The adaptive applicability function is an anisotropic Gaussian function which the main axis is rotated to adjust the orientation of the local dominant.

$$\alpha(s, s_0) = \rho(s - s_0) exp\left[-\left(\frac{x \cos \emptyset + y \sin \emptyset}{\sigma_u(s_0)} \right)^2 - \left(\frac{-x \sin \emptyset + y \cos \emptyset}{\sigma_v(s_0)} \right)^2 \right] \quad (10)$$

Where $s_0 = x_0$, 0 is the central of this analysis, $s - s_0 = x$ is the local coordinate input samples associated with s_0, while ρ is a pillbox function that centered at the origin which restricts the kernel to certain radius.

In equation (10), and are the scales of the Anisotropic Gaussian kernel is the scale that extends along the orientation and greater than or equal to σ_u. Then both scales are adjusted to the local scale σ_c.

$$\alpha_u = \frac{\alpha}{\alpha + A} \sigma_c \text{ and } \alpha_v = \frac{\alpha + A}{\alpha} \sigma_c \quad (11)$$

Parameters and functions used for high-resolution image reconstruction should use enough characteristic of image structure and detail of information, while the shape and size of the local neighborhood can be set adaptively.

Projection Onto Convex Sets (POCs) Algorithm: Another algorithm in image reconstruction that quite effective to improve the quality of image with blur and noise is POCs. POCs is not just a fairly simple algorithm, but it also can provide more detailed information of the reconstructed image. This algorithm is the iterative approach to perform the repetitive use of information from a series of low-resolution image and limiting the set of solutions to convex[14,15].

If a signal $f(x, y)$and the set of convex C_i assumed to be an element in Hilbert space, then $C_i \in H$ for $i = 1,2,\ldots,m$ and $f \in C_0 = \bigcap_{i=1}^{m} C_i$, provided that the slices in C_0 not zero. Given a set of constraints on C and the projection operator P_i in each $f(x, y)$ then obtained

$$f_{k+1} = Tc_m Tc_{m-1} \ldots Tc_1 f_k \quad (12)$$

Where the projection operator Pc_i is projecting the signal $f(x, y)$ to the set of convex C_i and λ_i is the multiplier with a value of $0 < \lambda_i < 2$.

Low-resolution image $g(x, y)$ used can be modeled as a high resolution image $f(x, y)$ that experienced a shift (s_x, s_y) and undergo a process of degradation or blurring by a point spread function $h(x, y)$ and the addition of noise $N(x, y)$ as the following equation:

$$g(x, y) = h(x, y) f(x + s_x, y + s_y) + N(x, y) \quad (13)$$

So that the set of equations is obtained convex C_i as follows:

$$C_i = \{f : ||g(x, y) - h(x, y) f(x, y)| \leq N(x, y)\} \quad (14)$$

Completion of the equation (14) is obtained by iteration of orthogonal projection to a convex set defined by the constraints of low-resolution image noise level, and then the projection operator which is obtained substituted into equation (12) to obtain the following equation:

$$f_{k+1} = f_k + \lambda_i \frac{g_i - h_i' f_k}{\|h_i\|^2} h_i^2 \quad (15)$$

g_i, is i th element of vector $g(x,y)$and $h_i'$is a line to i of matrix $h(x,y)$. An initial high resolution image called the image super resolution (SRI) is projected sequentially onto the set of constraints that are built around the components of the observation image $g(x,y)$ the so called low-resolution image (LRI). Projections made in the frequency domain.

Figure 2 shows an illustration of the POCs in the frequency domain. On the right side of the circuit depicted low resolution image (LRI), which through the process to define the image preprocessing is important and will be used in the reconstruction process, if all the image used then this process can be by passed.

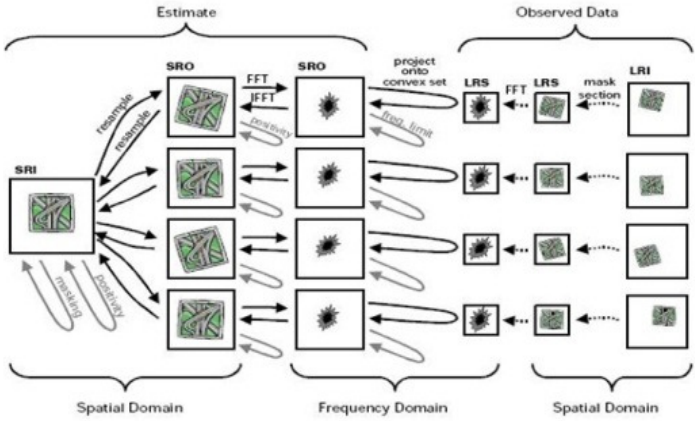

Figure-2
Illustration of POCs in the frequency domain

LRI to be used in the process of reconstruction in the Fourier transform into LRS. On the left is defined initial high-resolution image (SRI) obtained from the LRI which has been scaled or from a simple interpolation methods as nearest, bilinear, or bicubic. SRI in the re sample to adjust to the LRI, in this case when the rotation the LRI experience on SRI is also subject to rotation. SRI then transformed with a Fourier transform image super resolution overlay (SRO). SRO later in the projection in order to set constraints are defined using the LRS.

Material and Methods

In this research authors conducted a composite study between the registration and reconstruction process. The registration process used PBIM, while the reconstruction used two algorithms, such as SANC and POCs to find the best performance in producing high-resolution image. We fitted the data points around the peak point, to obtain more accurate shifting of the sub pixel. Block diagram in figure 3 is the stages that performed in this research. In this study, superresolution began with taking objects using video. They were extracted to obtain a series of images in the same scene. Then pixels translation was estimated using phased based image matching and fitted for the sub-pixel level shifting. In determining the effect of registration and reconstruction of objects which have different characteristics, we used some images that contain lots of texture and some other with less texture for experiment. The authors also compared the accuracy of the PBIM registration with fitting and Keren

This experiment was performed on an object that contains lots of textures and also ones with less texture. The purpose of this experiment was to get the best performance of composite between PBIM and Keren registration with SANC and POCs reconstruction algorithm POCs

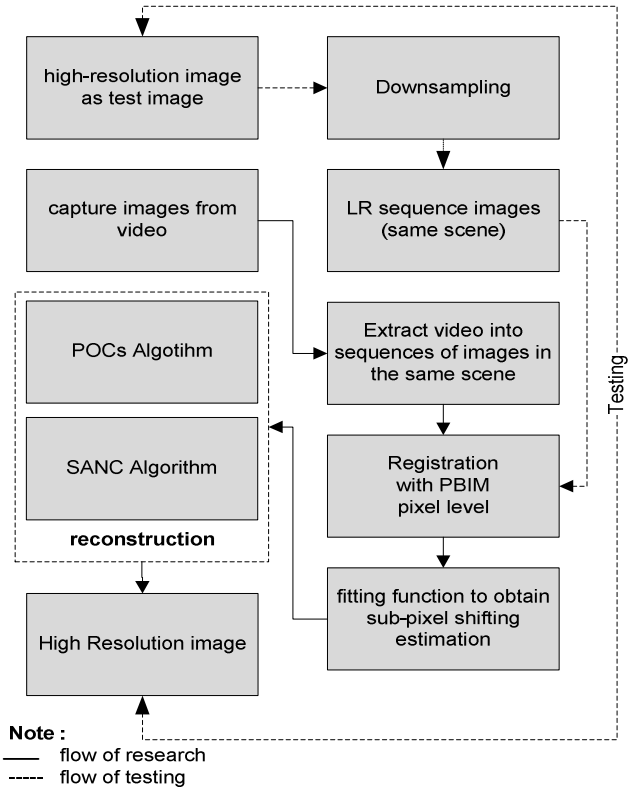

Figure-3
Block Diagram of Research

Figure-4
Test Images (a)image that contains lots of textures (b)image that contains less of textures

The scenarios of testing in this study are as follows : i. a test image in figure 4 was assumed to be a high-resolution image; ii. image downsampling was performed to obtain image with low

resolution; iii. in addition to lowering the resolution, downsampling also produced a number of image in the same scene; iv. a number of these images were registered using PBIM and Keren, then reconstruction of the registration was used to produce a high resolution image; v. finally, the results of this reconstruction was compared to the test images to obtain the value of PSNR.

Results and Discussion

Results of several experiments are discussed in the following section**.** Table 1 shows the PSNR values of image registration using composite of PBIM and reconstruction using two reconstruction algorithms, POCs algorithm and SANC algorithm. There are eleven experiment results from composite of two registration, PBIM and Keren registration algorithm with variant LR that contain lots of texture image. Table 1 also shows the highest average of PSNR that achieved in composite between PBIM registration with POCs algorithm and has PSNR average value of 32.558**.**

Table-1
PSNR results, image that contain lots of texture

Num of images	PBIM reg. With		Keren reg. with	
	POCs	SANC	POCs	SANC
4	31.1034	31.6416	31.1034	31.2356
6	31.8168	31.7715	31.4892	31.4827
8	31.9551	31.8389	31.4875	31.5248
10	32.247	31.7895	31.9551	31.3964
12	32.2469	31.7593	31.9551	31.3538
16	32.2458	31.8733	31.9541	31.441
20	32.2467	31.8967	31.9533	31.4449
30	32.2456	31.9691	31.8533	31.494
50	32.5517	32.2264	31.7114	31.7567
75	32.558	32.3337	31.7117	31.7562
100	32.5502	32.293	31.7118	31.7547
Avg	32.16065	31.94481	31.7169	31.5128

Composite between PBIM registration and SANC algorithm reconstruction has an average PSNR value of 32.16065, while Keren registration has lower PSNR value than the PBIM registration, for both construction algorithms. It shows that the registration PBIM is better than keren registration. Figure 5 presents a graph of the relationship between PSNR value and the number of reference image used for reconstruction. Image used in this experiment is an image that contain lots of texture.

While figure 6 shows the SR results using POCs reconstruction algorithm. From those figures, we can see that the images with less texture have average PSNR value lower than those with more texture. The results of this test are presented in table 2. This tabel shows a comparison between PBIM and Keren registration, which collaborated with the reconstruction algorithm POCs and SANC. This experiment uses images with less texture. The results show that PBIM registration with fitting function has a higher PSNR values compared with Keren registration, even for images with less texture.

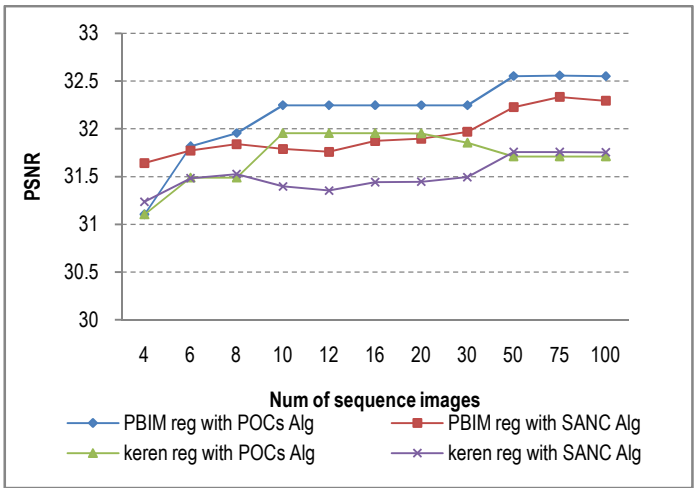

Figure-5
PSNR graph for image that contain a lots texture

(a) (b)

Figure-6
The results of SR, image that contain lots of texture
(a) input, (b) output

Table-2
PSNR results, images that contain less texture

Num of images	PBIM reg. with		Keren reg. with	
	POCs	SANC	POCs	SANC
4	29.5825	29.7528	29.0262	28.6641
6	29.4321	29.7761	29.0262	28.7287
8	29.8435	29.8306	28.7217	28.9435
10	29.8434	29.8926	28.7035	28.4784
12	29.8434	29.9063	28.7035	28.4516
16	29.8434	29.8894	28.7035	28.4524
20	29.8435	29.9971	28.6925	28.3821
30	29.9495	29.9195	28.6925	28.4049
50	29.9492	29.9116	28.6925	28.4558
75	29.9492	29.941	28.6947	28.5474
100	29.8448	30.2197	28.6947	28.4782
Avg	29.99313	29.91242	28.75922	28.54428

Figure 7 shows the relationship between PSNR value and various numbers of reference images, and composite between PBIM and various of construction algorithms. Figure 8 shows the SR results for image with less texture.

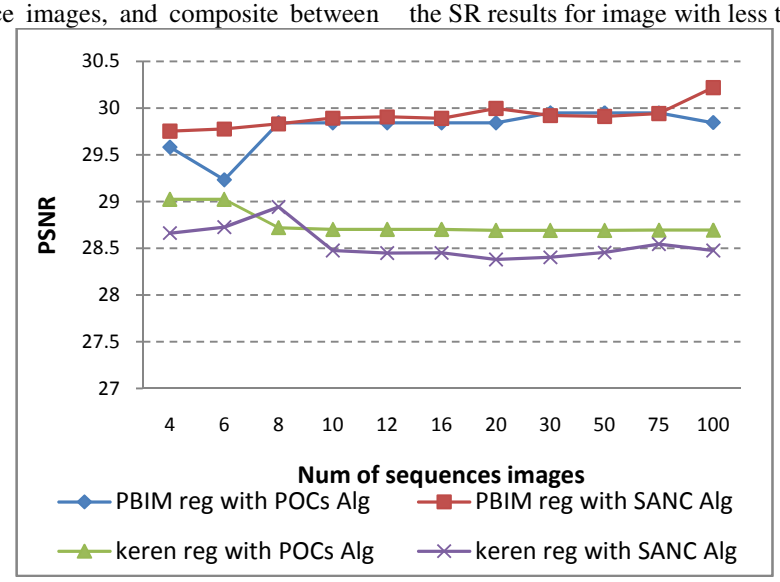

Figure-7
PSNR for image that contain less texture

(a) **(b)**

Figure-8
The results of SR, image that contain less of texture
(a) input, (b) output

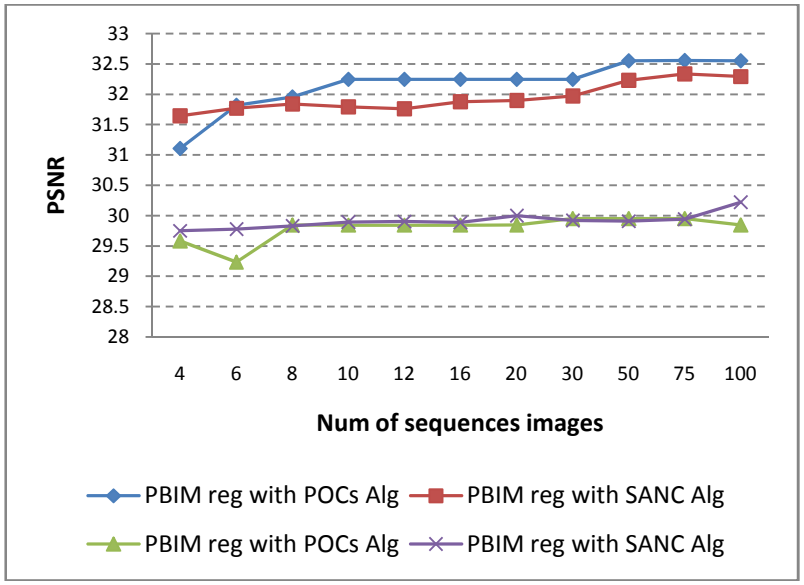

Figure-9
Performance of various reconstruction algorithms using PBIM registration

Figure 9 shows the perfomance of PBIM registration with two reconstruction algorithms for images with lots of texture and also for those with less texture.

Conclusion

Studies and experiments related to the composite between registration and reconstruction algorithm have been performed and obtained the following conclusions : i. In the experiment with a number of different reference images, the composite between PBIM registration and POCs reconstruction algorithms has the highest PSNR average of 32.160654, while the average value of PSNR for images with less texture is 29.912427, ii. Objects with less texture have lower average value of PSNR for every collaborative algorithms that have been tested in this experiment, iii. The result of PBIM registration with function fitting experiment has an average PSNR value of 2.88% higher than the Keren registration.

References

1. Sung Cheol Park, Min Kyu Park and Moon Gi Kang, Super-Resolution Image Reconstruction : A Technical Overview, *IEEE Sig. Proc. Magazine*, May **(2003)**

2. Z. Barbara, F Jan, Image registration methods: a survey, *Image and Vision Computing*, **(21)**, 977–1000 **(2003)**

3. Barreto D. and Alvarez Abad, Motion Estimation Techniques in Super resolution Imager Reconstruction, A Perfomance Evaluation, Virutal observatory: Plate Content Digitization and Image Sequence Processing **(2005)**

4. Kenji Takita and Takashumi Yoshisumi, High-Accuracy Subpixel image Registration Based on Phased Only Corelation, *IECE Trans Fund.*, **E86-A (8)**, **(2003)**

5. Kenji Takita and Muhammad Abdul Muquit, A Sub Pixel Correspondence Search Technique for Computer Vision Applications, *IECE Trans Fund.,* **E87(8),** Agustus **(2004)**

6. Hassan F. and Jossiane B.Z., Extension of Phase Correlation to Subpixel Registration, *IEEE Trans. on Image Proc.*, **11(3), (2002)**

7. Yi Liang, Phased Correlation motion Estimation, Final Project Stanford University **(2000)**

8. Mannuel G.Z., Thurman Samuel T. and Fienup James R., Efficient subpixel image registration algorithms, *Opt. Letters* **33(2),** 15 **(2008)**

9. Tiemao, Lin. and Xuyuan Zheng, Super-resolution Reconstruction of MR Image Based on Structure-adaptive Normalized Convolution, *ICSP IEEE* **(2010)**

10. Tuan Pham., Robust Fusion of Irregularly Sampled Data using AdaptiveNormalized Convolution, *EURASIP Journal on App. Sig. Processing* **(2006)**

11. Chong Fan, Jianjun Zhu, Jianya Gong and Cuiling Kuang, POCS Super-Resolution Sequence Image Reconstruction Based on Improvement Approach of Keren Registration Method, Sixth International Conference on Intelligent Systems Design and Applications (ISDA'06) isda, **2**, **(2006)**

12. Hong Yu, Ma Xiang, Huang Hua, Qi Chun, Face Image Super-resolution Through POCS and Residue Compensation, The Institution of Engineering and Technology, **(2008)**

13. BalamuralitharanS. and Rajasekaran S., Analysis of G-CSF Treatment of CN using Fast Fourier Transform, *Res. J. Recent Sci.,* **1(4)**, 14-21 **(2012)**